JOURNAL OF MATERIALS SCIENCE 24 (1989) 3541–3548

Stress relaxation in wood (Scots pine veneer)

D. G. KUBÁT, S. SAMUELSSON
Department of Building Materials, Royal Institute of Technology, S-100 44 Stockholm, Sweden

C. KLASON
Department of Polymeric Materials, Chalmers University of Technology, S-412 96 Gothenburg, Sweden

The kinetics of the stress relaxation process in Scots pine veneer with regard to the relation between the slope of the stress (ln time) curves and the initial effective stress, σ^* (applied minus internal stress) are analysed. The data obtained provide further support for the validity of the relation $F \approx 0.1\ \sigma_0^*$, with F denoting the above slope. This relation has been found to apply to a large variety of different materials, including metals, polymers, and others. The relaxation process was linear with regard to the initial stress. There was an increase in F in the final stage of the relaxation curves, apparently due to a different mechanism. This had to be taken into account when checking the validity of the above relationship between F and σ_0^*. The measurements relate to radially cut veneer samples at 50% relative humidity.

1. Introduction

In comparison with other materials, especially metals and plastics, the vioelastic properties of wood have not been studied in any great detail. Of course there are numerous investigations of creep in wood and wood structures; however, the evaluation of the results obtained is based on simplified, largely empirical engineering approaches without attention paid to possible molecular mechanisms governing such flow. With regard to stress relaxation, this situation is especially pronounced, only a limited number of publications dealing with this process being available in the literature.

From the physical point of view, the process of stress relaxation is significantly simpler than the process of creep. In the first place, this is due to the fact that stress relaxation in normal solids appears to be governed by a single type of flow. In creep, on the other hand, the primary, secondary, and tertiary stages of the process not only are difficult to separate from each other, but they also appear to depend on different mechanisms. The accelerating tertiary stage may be taken as an illustration.

Another significant feature of stress relaxation is the striking similarity between various solids with regard to the kinetics of this process. It has been amply demonstrated that the following formula is obeyed by solids with widely differing structures and chemical compositions, including metals, polymers, ionic solids, and many others [1, 2]

$$F = (0.1 \pm 0.01)\sigma_0^* \qquad (1)$$

Here, F denotes the maximum (inflexion) slope of the stress–ln time (t) curves and σ_0^* the initial effective stress, i.e. the applied (σ_0) minus the equilibrium stress, σ_∞, attained after sufficiently long times. Equation 1 is thus based on a simple analysis of $\sigma(\ln t)$ curves, normally showing a rectilinear portion covering two to three decades of time. It is the purpose of this paper to present a brief account of such an analysis carried out on pine veneer samples, and demonstrating that Equation 1 is obeyed also by this material. It may be added, however, that the samples used exhibited two dispersion regions which had to be separated in order to make the main region to comply with Equation 1.

Previous work on stress relaxation in wood can be summarized as follows. The observations of Kitazawa [3] appear to confirm the validity of the so-called logarithmic time-law, that is a linear relation between the decaying stress and logarithmic time. The coefficient m is the $\sigma = \sigma_1(1 - m \log t)$ relation, with σ_1 denoting the stress (compression) after one minute and t the time in minutes, seems to vary in inverse proportion to the density of the wood sample. Some ten species, mainly North American, both coniferous and deciduous, were measured, the values of m varying between 0.0178 (Alaskan cedar, density 0.45 g cm^{-3}) and 0.069 (Quebracho, 1.12 g cm^{-3}). About the same m value was found for Compreg. The measuring time was about 10 h.

The data of Campredon [4] show that the stress exerted by the ends of a bent pine board decreased by about one-third after 150 d under constant deformation. In a linear $\sigma(t)$ plot, the relaxation curve shows a slow-down in the final stage of the flow process.

Grossman [5] points out the inadequacy of Kitazawa's log t formula for extended measuring periods. Studying specimens of hoop pine in the bending mode he found that after the initial linear log t portion, the relaxation curves showed a sigmoid inflexion region covering about a decade of time, the inflexion appearing at 10^3 to 10^4 min. There were indications of an approach to

0022–2461/89 $03.00 + .12

a stress equilibrium after passing through this region. The measuring time was up to 5×10^6 sec (2 mon). A comparison of similar data with creep is presented by Grossman and Kingston [6] who report that departures from linear viscoelasticity are small in dry wood (hoop pine), the relaxation and creep curves forming mirror images of each other when suitably normalized. Again a pronounced sigmoid inflexion is found after 10^3 to 10^4 min, encompassing the main portion of the stress decrease due to relaxation, and extending approximately over one decade of time, thus reminiscent of a Maxwellian process. A relatively good fit was achieved using a sum of three exponentials. The sigmoid inflexion noted both in relaxation and creep was absent in the corresponding creep recovery curves. The humidity of the measuring room was not controlled.

Similar results are reported in a subsequent paper of the authors [7], again relating to "commonly prevailing conditions of ambient temperature and humidity". When comparing creep and relaxation data, Boltzmann's principle of superposition was found to be valid up to stresses approaching the fracture level. The limit of linear behaviour was lowered by high humidity and also by the presence of compression wood in the samples. Some of the creep experiments were carried out in tension and shear while the relaxation data relate to bending. The measurements covered a period of about 2 mon.

An exploratory study of the relaxation process in compression in the longitudinal-tangential plane of Douglas fir is presented by Bach and Rovner [8]. The extent of relaxation was found to increase with the grain angle. The measurements extended over a period of about 100 min.

Fracture during the relaxation process (static fatigue) was studied by Bach [9] for Douglas fir and spruce loaded along the grain. The probability of fracture for different times under load (1 to 10^3 min) was determined. This work is continued in a subsequent paper [10]. The author concludes that the time constants characterizing the stress decay of earlywood and latewood of Douglas fir are approximately equal.

Relaxation in compression and tension for specimens of six American tropical species are compared by Echenique-Manrique [11]. Compression resulted in a more extensive flow than tension. The measuring time was 8 h, the initial strain 0.1 to 0.5% in compression, and between 0.15 and 0.8 to 0.9% in tension. In compression, the stress decrease in 8 h ranged from a few per cent at the lowest initial strain to 30 to 40% at the 0.5% strain level, thus indicating a strongly non-linear behaviour. In samples loaded extensionally the stress fell only a few per cent at low strains, this figure increasing to 7 to 9% for certain specimens strained initially to 0.8 to 0.9%. The results were obtained at room temperature and 65% relative humidity (r.h.). Using a three element model, the author finds that Eyring's theory (stress dependent thermal activation, see below) fits the experimental results. Apart from the relatively short measuring time, some of the relaxation curves show an indication of stress equilibrium in their final stage.

Relaxation in bending and torsion of Hinoki wood specimens during sorption of water vapour is the subject reported in [12]. At constant humidity, the $\sigma(t)$ curves showed distinct signs of an approach to stress equilibrium. Upon a stepwise increase in humidity of the surrounding atmosphere, an additional relaxation process was recorded, bringing the relaxation modulus to very low values. The effects observed were similar to those known to occur in creep under cyclic humidity changes (e.g. [13]). The authors conclude that their results do not constitute a sufficient basis for an explanation of the accelerating effect of a humidity change on the flow rate.

Relaxation in torsion of Hinoki wood impregnated with poly(ethylene oxide) was slower than in untreated specimens kept at 20% r.h. The measuring time was too short to allow the kinetics of the process to be analysed [14].

The relaxation behaviour of cork in compression has been measured by Dart and Guth [15] at temperatures between 30 and 200° C. The measuring period was a few hours, the stress being determined with a chain balance. Perfect linearity of the $\sigma(\log t)$ plots was observed at all temperatures and stresses, the latter corresponding to compressions between 2 and 60%. Extrapolation of the $\sigma(\log t)$ curves yielded a family of straight lines intersecting in a common point on the log t axis (4.5×10^8 min at 31° C), thus indicating linear behaviour. It is interesting to note that the $\sigma(\log t)$ curves scaled linearly with regard to σ_0, despite the fact that the σ_0 values covered a significant portion of the sigmoid stress–compression curve of cork, and that considerable destruction of the cell walls must have taken place at the highest compression levels. The extrapolated decay time to $\sigma = 0$ decreased with increasing temperature.

The work on stress relaxation in wood, as discussed above, is hardly amenable to a quantitative evaluation. This is due, in the first place, to the complex loading modes used and, in many cases, also to absence of a humidity control.

2. Theoretical background

There are two main lines of approach when describing stress relaxation phenomena in solids, the theory of relaxation time spectra (RTS), and the theory of stress-dependent thermal activation (SDTA). The concept of RTS is equivalent to that of linear viscoelasticity [16]. It is a purely formal approach describing the process in terms of a spectrum of Maxwellian relaxation times, because, as well known, a single Maxwellian mechanism is far from sufficient to describe the experimental facts. Instead, a rather broad spectrum is required. According to RTS, the time dependence of the stress is given by the following expression

$$\sigma(t) = E\varepsilon_\infty + \varepsilon_0 \int_{-\infty}^{\infty} H(\tau) e^{-t/\tau} \mathrm{d} \ln \tau \qquad (2)$$

where $H(\tau) = \tau E(\tau)$ is the distribution of relaxation times τ, E the modulus (unrelaxed, initial), and ε_0 and ε_∞ the initial and ultimate (recoverable) deformation, respectively. $E(\tau)$ denotes the contribution of flow mechanisms with relaxation time τ to the process; $H(\tau)$

is the corresponding quantity with regard to ln τ. The use of the latter distribution function is motivated by the fact that relaxation curves are normally plotted as $\sigma(\log t)$.

Since the connection between $H(\tau)$ and the physical mechanisms taking place in the relaxing solid is not known, the RTS approach is purely formal, replacing $\sigma(\tau)$ with the corresponding spectral density curve. In normal solids, $H(\tau)$ is approximately box shaped, the τ-values being confined with about equal density to a limited portion of the ln τ axis. Such a distribution is equivalent to a linear $\sigma(\log t)$ relation as normally observed in experiments. On the other hand, the shape of the $\sigma(\log t)$ plot is not very sensitive to the form of the τ-distribution.

The second major line of approach when discussing flow in solids is the SDTA concept (e.g. [17]). In the case of stress relaxation, it can be formalized in an especially simple way, i.e.

$$-\dot{\sigma} = \mathrm{d}\sigma/\mathrm{d}t = A' \exp\left[-(\Delta G - v\sigma/kT)\right] = A \exp\left(v\sigma/kT\right) \quad (3)$$

where ΔG is the activation energy which the flow units have to accumulate by thermal activation in order to surmount the potential barriers inhibiting their free movement, k is the Boltzmann constant, T the temperature, v the activation volume, A, and A' the so-called pre-exponential factors. This relation is based on the notion that the activation energy is diminished by the elastically stored energy, $v\sigma$, due to initial strain. In itself, Equation 3 is the Boltzmann expression for the probability that a flow unit, or any microscopic part of the solid under consideration, attains a certain energy by thermal fluctuations.

In its integrated form, Equation 3 reads

$$\sigma(t) = \frac{kT}{v} \ln\left[B + (A\, v/kT)t\right] \quad (4)$$

with $B = \exp(-v\sigma_0/kT)$. As can be seen, this formula also yields a $\sigma(t)$ relation linear over a significant period of time when plotted in a $\sigma(\log t)$ diagram.

According to Equation 4, the maximum (inflexion) slope F of the $\sigma(\ln t)$ plot, i.e. F, is given by

$$F = kT/v \quad (5)$$

As shown below, because F scales linearly with the initial stress σ_0, and also, according to Equation 1, with σ_0^*, v is expected to vary inversely with these quantities.

As a rule, $\sigma(\log t)$ plots show a rectilinear portion covering a few decades of time. The equilibrium stage, characterized by the attainment of the σ_∞ stress level, is normally not included in the experiments, mainly due to the long measuring times required to reach the equilibrium stage, and also to difficulties in maintaining the stability of the equipment during such time periods. After passing the σ_∞ stage, the process may continue by a different mechanism, resulting in a further decrease of σ. Experimental data exhibiting such effects will be presented below.

The slope F is a central parameter in both RTS and SDTA. In RTS, it defines the spectral density of the spectrum according to the formula [16]

$$H(\ln \tau) \approx F/\sigma_0^* \quad (6)$$

Equation 5 is a first approximation, higher derivatives of $\sigma(t)$ with regard to log t giving higher approximations. However, in normal cases, the quality of the relaxation curves does not allow the use of higher derivatives. A box spectrum, often depicting experimental facts with sufficient accuracy, is thus defined by F.

The second main parameter of interest here is the equilibrium stress, σ_∞, also called internal stress, required when checking the validity of Equation 1. As already mentioned, this quantity is not easily amenable to measurement, which also explains the fact that the similarity between different materials expressed by Equation 1 often eludes experimental observers.

3. Experimental details

3.1. Material

The samples used were taken from radially cut splint veneer of Scots pine (*Pinus silvestris*) having a thickness of 0.75 to 0.80 mm. The distance between the growth rings was 1.4 ± 0.1 mm, the proportion of latewood 24 ± 3%. The density was 0.490 g cm^{-3} at 50% r.h.; the humidity content was 5.9%.

The effective length of the rectangular samples was 6 cm; their width was 3, 6, and 12 mm (cf. Table I).

3.2. Relaxation measurements

The measurements were carried out with equipment similar to that described in [18]. The stiffness of this equipment was determined by measuring the combined movement of the stress-sensing membrane and that of the straining device, the latter being based on a micrometer screw with a pitch of 0.5 mm. The total deflection measured was negligible compared to the deformations used; the equipment can thus be considered as ideally stiff, and corrections are not necessary. It may be added that the value of F/σ^*, as appearing in Equation 1, does not depend on machine stiffness.

The deflection of the stress-sensing circular membrane was determined using an inductive transformer (Vibrometer TS/1230) connected to a carrier frequency (8 kHz) bridge (Vibrometer 8-ATR 1/S). The deformation rate used in the initial straining of the samples was 0.5 and 0.042 mm sec^{-1}, corresponding to a strain rate of 8.3×10^{-3} and 7.10×10^{-4} sec^{-1}, respectively.

The relaxometer was placed in a closed cabinet in order to equalize humidity fluctuations in the measuring room, which was conditioned to 50 ± 3% r.h.

When evaluating the relaxation curves, the time was measured from the end of the straining period (given in Table I). Because the strain–strain curves were virtually linear, the initial strain may be obtained from the strain rate and the straining time. Normally, the measuring time was 1 to 2 d. The curves shown in Fig. 3 exemplify the period of measurement.

When calculating the length of the straining period, the initial curvature of the stress–strain curve was corrected for, c.f. Table I.

4. Results

As already mentioned, the emphasis in reproducing the results obtained is on the determination of the

TABLE I The values of $F/\Delta\sigma$ and other parameters of a selection of typical stress relaxation curves measured on longitudinal (L), transverse (T), and 45° samples. t_1 denotes the straining time. The strain rate was $7.0 \times 10^{-4}\,\mathrm{sec}^{-1}$ for the L-samples, the 45°-sample 12, and for the T-samples 13 to 16. The 45° sample 11 and the T-samples 17 to 21 were deformed at $8.3 \times 10^{-3}\,\mathrm{sec}^{-1}$. The data compiled in this table constitute only a part of the experiments reproduced in Figs 1 and 2. The average of $F/\Delta\sigma$ is 0.099 ± 0.009 in accordance with Equation 1

No.	Orientation	Sample width (mm)	$F/\Delta\sigma$	F/σ_0 ($\times 10^{-2}$)	$\Delta\sigma/\sigma_0$	σ_0 (MPa)	t_1 (sec)
1	L	6	0.100	0.60	0.060	6.2	1.05
2	L	6	0.109	2.57	0.235	8.4	1.68
3	L	6	0.099	1.52	0.154	8.2	1.50
4	L	6	0.101	1.31	0.129	16.7	3.23
5	L	6	0.110	1.37	0.125	18.0	2.82
6	L	6	0.102	1.26	0.123	18.6	2.90
7	L	3	0.108	1.08	0.100	32.2	5.25
8	L	3	0.086	1.42	0.165	35.6	5.61
9	L	3	0.091	1.61	0.176	36.7	5.67
10	L	12	0.097	1.46	0.148	37.5	5.64
11	45°	6	0.092	2.22	0.241	2.82	0.83
12	45°	6	0.116	1.86	0.16	0.935	2.43
13	T	6	0.109	2.75	0.252	0.627	4.7
14	T	6	0.105	3.07	0.292	0.650	4.8
15	T	6	0.098	3.48	0.355	2.02	16.3
16	T	6	0.103	3.56	0.345	3.01	25.5
17	T	12	0.095	1.96	0.207	0.79	0.72
18	T	12	0.086	2.61	0.304	0.87	0.74
19	T	12	0.084	2.07	0.247	1.26	1.40
20	T	12	0.085	2.34	0.276	1.66	1.15
21	T	3	0.099	2.85	0.288	1.85	1.14

general shape of the relaxation curves as given by the slope F and the value of σ_∞.

4.1. The linearity of $F(\sigma_0)$

Fig. 1 shows the variation of F with the initial stress, σ_0 for three different sample orientations, 0°, 45° and 90° to the grain. The slope of the $F(\sigma_0)$ lines increases in that order, showing that the extent of the stress decay due to relaxation is largest in the transverse (tangential) direction. This is in agreement with the data given in [8]. An important feature of these graphs is their linearity. Disregarding possible shifts along the log t axis (although difficult to estimate they do not appear to be important in this context) we thus find that the slope F scales linearly with σ_0, the wood samples used behaving as a linear viscoelastic solid.

The SDTA theory, as expressed by Equation 3, predicts an exponential dependence between $\dot{\sigma}$ and σ, a fact which can be reconciled with these results only by assuming an inverse relation between σ_0 and the activation volume. This will be commented on below.

Although the $F(\sigma_0)$ points in Fig. 1 arrange themselves well along their respective lines, they show a somewhat larger scatter than normally observed with other solids. An obvious reason for this appears to be the heterogeneous structure of the samples, the scale of the heterogeneities being of the same order as sample dimensions. For instance, the number of growth rings may vary, at the same time as there may be some variation in orientation relative to the grain. We have not analysed these factors any closer, because they do not affect the conclusions drawn from the results.

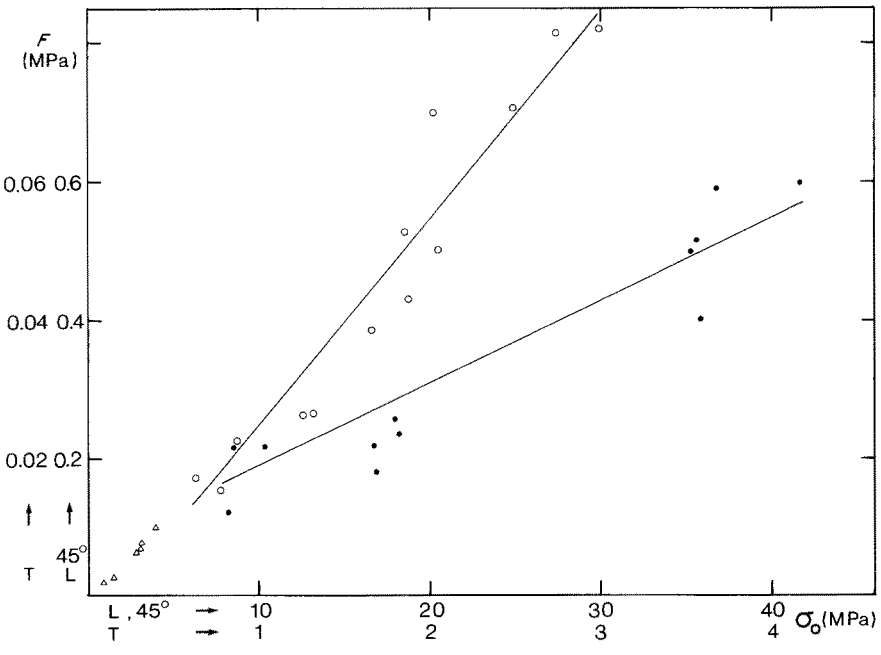

Figure 1 The slope, F of $\sigma(\ln t)$ against σ_0 for (●) longitudinal, (○) transverse and (△) 45° samples. Solid lines calculated by regression.

TABLE II

Direction	E (GPa)
Longitudinal	9.7 ± 1.4
45°	0.57 ± 0.15
Transverse	0.20 ± 0.05

The scatter of the $F(\sigma_0)$ points shown in Fig. 1 was also reflected in the calculations of the modulus E as evaluated from the slope of the $\sigma(\varepsilon)$ curves. In most cases these curves were practically linear. Due to structural inhomogenities of the samples there was an inevitable variation in the E values, which were as given in Table II. The value of E was not influenced significantly by the change of the strain rate from 8.3×10^{-3} to 7.0×10^{-4} sec^{-1}, neither had variation of sample width any influence (3, 6, and 12 mm wide samples).

4.2. The validity of Equation 1

The main result of the present investigation is summarized in Fig. 2 which demonstrates that plotting F against σ^* gives a straight line in perfect agreement with Equation 1. It is also interesting to note that the scatter in this case is significantly below that found in the corresponding $F(\sigma_0)$ diagrams, Fig. 1.

The plot in Fig. 2 is based on the initial effective stress $\sigma_0^* = \sigma_0 - \sigma_\infty$, which in turn, requires the determination of the equilibrium stress, σ_∞. As in all relaxation studies, this represents the most difficult part of the measurement. Apart from normal problems with the stability of the equipment, we also have an additional complicating factor in the fluctuations of the humidity of the surrounding atmosphere. Such fluctuations result in dimensional changes of the sample which, in turn, may yield apparent changes in the recorded stress, thus obscuring the true course of the relaxation process.

While no difficulties are encountered in determining the value of F, assessment of σ_∞ cannot be made without a certain degree of ambiguity. The main reason for this is that the specimens used exhibited a distinct approach to equilibrium in a few cases only, the bulk of the curves showing a final stage, linear in the $\sigma(\log t)$ plot, but with a higher slope than the main relaxation region from which the value of F was determined. Some typical examples of the shape of the relaxation curves are shown in Fig. 3.

With regard to defining σ_∞, the following point may be noted. When a single relaxation region only is present, we consider the measuring times to be sufficiently long to consider the last σ value as σ_∞, even though a true equilibrium has not been attained, that is when σ still shows a decreasing trend. Previous experiments with paper [18, 19] have demonstrated, that the error incurred in this procedure lies well within the scatter specified in Equation 1. When a slight fluctuation in σ is present, the final σ value is averaged over a period of time.

When two relaxation mechanisms (dispersion regions) are present, which was the rule in the present case, we assume that the σ value corresponding to the main relaxation can be obtained by graphical separation of the two processes using intercepts of straight line extrapolations, cf. Fig. 3. A similar procedure is used when the two processes follow each other with an intermediate inflexion.

The results of this evaluation are reproduced in Table I, where the total stress decrease due to the main relaxation process is denoted $\Delta\sigma$. This quantity is close to $\sigma^* = \sigma_0 - \sigma_\infty$, even though a true equilibrium has not been attained, cf. the final stage of the $\sigma(\log t)$ curves shown in Fig. 3. The verification of the validity of Equation 1 is thus based on the use of $\Delta\sigma$, the ratio $F/\Delta\sigma$ in fact being approximately 0.1 as is evident from Table I. Only curves extending over a sufficiently long period of time, exhibiting either an approach to equilibrium or a distinct transition to another relaxation mechanism in their final stage, were used in evaluating the value of $F/\Delta\sigma$ as given in Table I. An additional requirement was the absence of disturbances in the curve shape due to temporary malfunction of the electronic equipment or the conditioning unit.

4.3. Internal stresses

As already mentioned, the internal stress, σ_i, entering

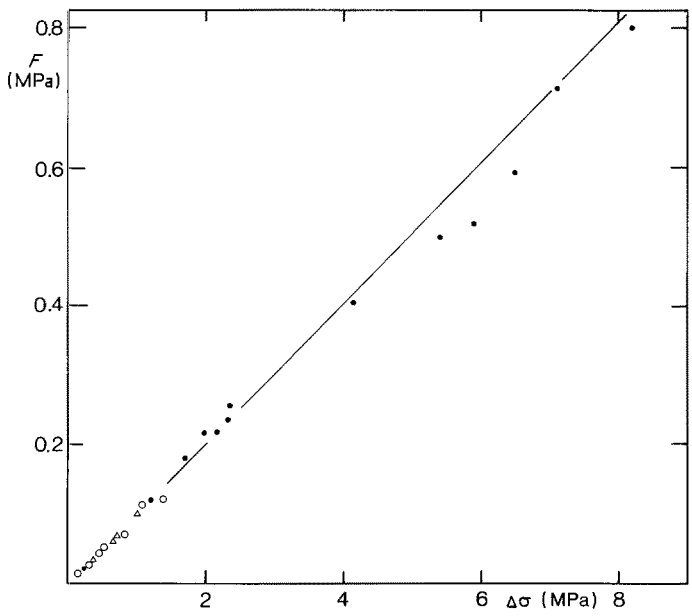

Figure 2 The slope F of $\sigma(\ln t)$ against $\Delta\sigma$ for (●) longitudinal, (○) transverse and (△) 45° samples. The quantity $\Delta\sigma$ is the difference between the initial stress and the apparent ultimate stress of the primary relaxation region determined according to the scheme illustrated in Fig. 3. The solid line corresponds to $F = 0.1\Delta\sigma$, Equation 1.

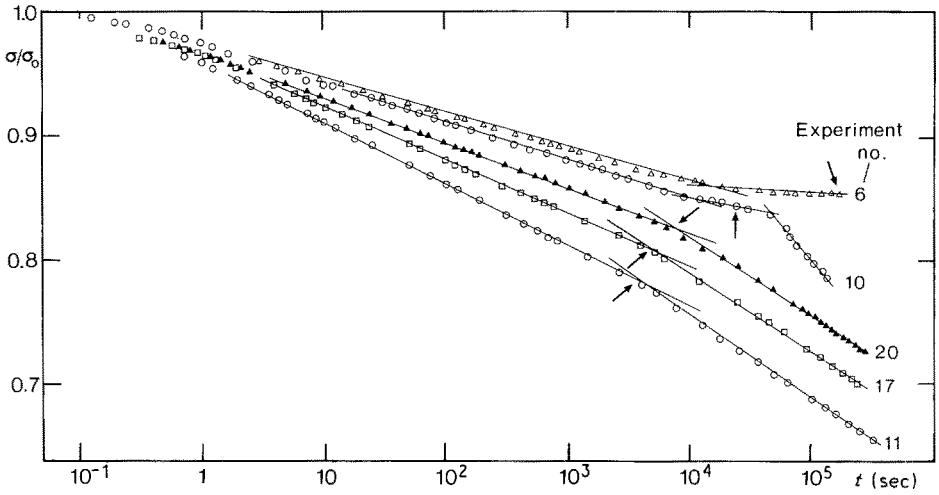

Figure 3 Examples of typical relaxation curves plotted as σ/σ_0 against log t. Arrows indicate the points where the apparent σ_x value was taken (cf. text). The numbers refer to Table I where the experimental conditions are specified.

the expression $\sigma^* = \sigma - \sigma_i$, defining the effective stress, is equal to the equilibrium stress in a relaxation measurement. When the applied stress σ falls to the σ_i level, σ^* decreases to zero and the flow process is terminated. This is in agreement with the generally accepted assumption that the flow rate is determined by the effective stress. Since the $\sigma(\log t)$ curves scale linearly with respect to σ_0, as evident from the linearity of the $F(\sigma_0)$ relationship, it follows from Equation 1 that also $\sigma_i (= \sigma_\infty)$ depends linearly on σ_0, or, indirectly, on the initial deformation of the sample. In order to distinguish this quantity from permanent internal stresses, to be discussed below, we denote it σ_{id}.

Because the direct determination of σ_{id} requires the experimentally difficult attainment of a stress equilibrium, Li [20] has devised an approximation method based on the extrapolation of the $(d\sigma/d \log t)$ against σ curves to zero stress. This procedure appears to work well provided the final part of the relaxation curves, where the actual extrapolation is carried out, obeys a power law expression, i.e.

$$\dot{\sigma} \sim (\sigma - \sigma_i)^n \tag{6}$$

giving a straight line to be extrapolated. With certain solids such as, for instance, polyethylene [21] this method gives reliable results. We refrain from applying Li's procedure because the relaxation curves obtained do not appear to behave in the above way.

It is further to be noted that in the present case the significance of σ_{id} is restricted to the main dispersion region only. The meaning of this parameter as a limit to further flow has to be modified correspondingly.

Apart from σ_{id}, the relaxation method also allows determination of another internal stress level, that is the quantity σ_{ir} which denotes the permanent level of internal stresses introduced, for instance, during the production process. The magnitude of σ_{ir} is determined as the intercept of the $F(\sigma_0)$ lines with the σ_0 axis [21]. As amply demonstrated in the literature, σ_{ir} varies in accordance with experimental conditions known to influence the internal stress level. In paper, for instance, drying under mechanical constraint yields a σ_{ir} value which increases with the drying stress [18]. Similar results have been recorded with polyethylene samples cooled from elevated temperatures under stress [21]. The magnitude of σ_{ir} thus appears to be a measure of permanently dried-in or frozen-in stresses.

In the present case, Fig. 1 shows that the value of the intercept defining σ_{ir} is larger for the longitudinal samples than for the two others. We simply state this without going into detail regarding possible interpretations of this result. The scatter of the data in Fig. 1 is another reason for this.

The above definition of σ_{ir} as the intercept of $F(\sigma_0)$ with the σ_0 axis obviously implies that no flow can take place at stresses lower than σ_{ir}. However, this should be considered with some care, because the $F(\sigma_0)$ may change its slope at the lowest stresses. In Fig. 1, such a change is not evident, the σ_{ir} values being rather low.

5. Discussion

Although the present work may be characterized as being of a rather preparatory nature, it nevertheless shows that Equation 1, previously found to be valid for a wide variety of solids, also holds for the complicated structure exhibited by the wood samples studied here. Apart from specifying the numerical value of the slope of the $\sigma(\ln t)$ curves, it also points to another important feature of stress relaxation, that is its linear scaling with regard to the initial stress. In this connection, it may be appropriate to comment in some detail on this linearity which apparently has been the reason for some confusion in the past.

A stress relaxation plot which is linear over a significant range in a $\sigma(\log t)$ diagram corresponds to an exponential relation between $\dot{\sigma}$ and σ

$$\dot{\sigma} \sim \exp \alpha\sigma \tag{7}$$

where α is a constant. Because relaxation curves normally exhibit the $\sigma(\log t)$ type of linearity, it is not surprising that the SDTA concept became a commonly accepted tool in describing such phenomena. However, one seems not to have noticed that the SDTA theory cannot distinguish between the role played by $\sigma(t)$ and σ_0. With regard to $\sigma(t)$, Equation 4 apparently describes the linear $\sigma(\log t)$ variation as observed in experiments. When it comes to the linear scaling of

the $\sigma(\log t)$ curves upon changing σ_0, the SDTA approach fails for obvious reasons.

An application of the SDTA formula [3] to a process scaling linearly with σ_0 gives an inverse type relation between the activation volume and σ_0. Due to the validity of Equation 1 this relation, relating to the first dispersion region of the curves, reads

$$v = 10kT/\sigma_0^* \tag{8}$$

It is to be stressed that Equation 8 is valid for all solids obeying Equation 1; attempts to relate the magnitude of the activation volume to certain geometrical features of the relaxing structure thus appear highly questionable. Ferguson and Yew [22] report a constant value of v for low stresses, whereas an inverse type relation between v and σ is found for higher stress values. The data are based on the application of the SDTA model to the yielding of several types of wood, the value of v being associated with the size of the cellulose microfibrils which are considered as the primary flow units. The physical meaning of v is not that of the volume of a structural unit; instead, v relates to the volume of the surroundings of that unit involved in its rearrangement.

When applied to the RTS concept, Equation 1 defines the width of the τ-spectrum. In the simple case of a box spectrum, the width becomes 4.3 decades of τ, in agreement with the findings presented above.

The RTS model is often related to a distribution of activation energies, U_i, through

$$\tau_i \sim \exp(U_i/kT) \tag{9}$$

Combining this with Equation 1 gives $10kT$ as the width of the distribution of U_i. Due to the uncertain nature of the assumptions underlying the RTS and SDTA concepts we refrain from further comment on this result here. The same applies to Equation 8.

For the sake of completeness it may be mentioned that various types of power law expressions are being used in order to describe the kinetics of creep in wood and wood structures, often in combination with simple mechanical models [23]. However, in the present case such an approach cannot be taken due to the linearity of $\sigma(\log t)$. Neither can Li's method [20] for the evaluation of internal stresses from relaxation data be applied, because it is based on an extrapolation of a power law region of such curves.

A proposal [24] is to factorize Equation 3 to read

$$\sigma \sim \exp[\Delta G(\sigma_0^*)/kT][\exp(\sigma^*/F) - 1] \tag{10}$$

in order to accommodate the dual nature of σ_0 and $\sigma(t)$. However, neither this equation, nor its original version, can provide an explanation of the peculiar similarity between various solids as expressed by Equation 1. Furthermore, the physically appealing background of Equation 3 is lost in the modified form, and the origin of the logarithmic time law remains unexplained. As already mentioned, the RTS concept is a formal approach only, not giving any connection with possible physical mechanisms behind the process.

During recent years, a cooperative approach to stress relaxation has been proposed [25]. It starts from the assumption that the elementary processes constituting the macroscopic process are not independent of each other, as in the SDTA theory, but coupled. The coupling mechansim, roughly equivalent to Bose–Einstein statistics, implies that a spontaneously initiated event may induce any number of other events to take place simultaneously.

Such a mechanism yields a time process of the type

$$\dot{\sigma} \sim \frac{1}{e^{kt} - 1} \tag{11}$$

which, for small values of kt approximates to $\dot{\sigma} \sim 1/t$ or $\sigma \sim \log t$, which is in agreement with experimental facts. Needless to say, also $\dot{\sigma} \sim \exp \alpha\sigma$ is obtained. Because Equation 11 can be considered as the result of a superposition of microscopic events of varying multiplicity (clusters), it is basically a spectral formula easily linearized with respect to σ_0. An important feature of Equation 11 is that it appears to be bounded in a way limiting the maximum cluster size to values yielding Equation 1, cf. [26]

It is also worth mentioning that the stretched exponential $\exp(kt^\beta)$, which has become a frequently used tool in describing time dependent processes, appears to fit into the pattern outlined by Equation 1. It is frequently observed that the value of the parameter β, giving the extension of the curves in $\log t$ diagrams, is around 0.25 to 0.35. This is in agreement with Equation 1 which requires that $\beta = 0.27$ $(= e/10)$ when calculating the slope from plots based on $\exp(kt^\beta)$. Experimentally, as a rule, such plots cannot be distinguished from $\sigma(\log t)$ diagrams when the constants are properly adjusted [27].

Despite the rather limited experimental material available, it has been possible to demonstrate that the wood samples used here fit the general pattern of relaxational behaviour found with other solids and manifesting itself in the form of Equation 1. With regard to the general shape of the relaxation curve, the transition to a $\sigma(\log t)$ region with a higher slope in the final portion of such curves certainly represents a feature recorded only in very few instances. In certain metals, such as lead or tin, such behaviour can be due to recrystallization, although in the case of tin a similar pattern was exhibited also by single crystals [28]. Another instance is that of rapidly quenched low-density polyethylene samples, where such an effect could be due to redistribution of internal stresses [28]. In the present case, the similarity of the observed behaviour with that of anisotropic (machine made) paper is especially interesting [18, 19]. Also the increase in the slope of the $\sigma(\log t)$ plots in their final stage for wool fibres, as reported in [29], may be mentioned.

It may be speculated that the occurrence of two dispersion regions in wood and paper, both appreciably hygroscopic, is associated with diffusion effects. In view of the significant effect of humidity changes on the creep of wood [13], one cannot exclude the possibility that the second dispersion region is related to the fluctuations of the conditioning unit.

Considering the fact that stress relaxation in wood normally encompasses two dispersion regions, the stability of the ratio $F/\Delta\sigma$, Equation 1, relating to

the initial region of the curves, appears even more remarkable.

Acknowledgements

The authors thank Professor K. Ödéen, Royal Institute of Technology, and the Swedish Board for Technical Development for supporting this investigation.

References

1. J. KUBÁT, *Nature* **204** (1965) 378.
2. J. KUBÁT and M. RIGDAHL, *Mater. Sci. Engng* **24** (1976) 223.
3. G. KITAZAWA, NY State College Forestry, Syracuse, New York, Tech. Publ. No. 67 (1947).
4. M. J. CAMPREDON, Inst. Tech. Batiment Trav. Publ., Circulaire Ser B, No. 23 (1947).
5. P. U. A. GROSSMAN, *Nature* **173** (1954) 42.
6. P. U. A. GROSSMAN and R. S. T. KINGSTON, *Austral. J. Appl. Sci.* **5** (1954) 403.
7. *Idem, ibid.* **14** (1963) 305.
8. L. BACH and B. ROVNER, Forest Prod. Lab. Vancouver, British Columbia, Inform, Rep. VP-X-14, 1967.
9. L. BACH, *ibid.*, VP-X-24, 1967.
10. L. BACH, *Wood Sci.* **3** (1970) 31.
11. R. ECHENIQUE-MANRIQUE, *Wood Sci. Technol.* **3** (1969) 49.
12. H. URAKAMI and M. FUKUYAMA, *J. Jpn Wood Res. Soc.* **15** (1969) 71.
13. D. G. HUNT and C. F. SHELTON, *J. Mater. Sci.* **22** (1987) 313.
14. T. SADOH and H. URAKAMI, *J. Jpn Wood Res. Soc.* **13** (1967) 323.
15. S. L. DART and E. GUTH, *J. Appl. Phys.* **17** (1946) 314.
16. A. V. TOBOLSKY, "Properties and Structure of Polymers", (Wiley, New York, 1960).
17. A. S. KRAUSZ and H. EYRING, "Deformation Kinetics" (Wiley Interscience, New York, 1975).
18. F. JOHANSON and J. KUBÁT, *Svensk Papperstidn.* **67** (1964) 822.
19. F. JOHANSON, J. KUBÁT and C. PATTYRANIE *Arkiv Fysik (Sweden)* **28** (1964) 317.
20. J. C. M. LI, *Can. J. Phys.* **45** (1967) 493.
21. J. KUBÁT, M. RIGDAHL and R. SELDÉN, *J. Appl. Polym. Sci.* **20** (1976) 2799.
22. W. G. FERGUSON and F. K. YEW, *J. Mater. Sci.* **12** (1977) 264.
23. C. B. PIERCE *et al., Wood Sci. Technol.* **19** (1985) 83.
24. H. CONRAD, *Acta Metall.* **6** (1958) 339.
25. C. HÖGFORS, J. KUBÁT and M. RIGDAHL, *Phys. Status Solidi B* **107** (1981) 147.
26. J. KUBÁT, *ibid.* **111** (1982) 599.
27. C. G. EK, J. KUBÁT and M. RIGDAHL, *Colloid Polymer Sci.* **265** (1987) 803.
28. J. KUBÁT, DSc Thesis, University of Stockholm, 1965.
29. E. T. KUBU, *Textile Res. J.* **22** (1952) 765.

Received 15 August 1988
and accepted 11 January 1989